Effect of external stress on discontinuous precipitation in a Cu-2.1 wt % Be alloy

Effect of external stress on discontinuous precipitation in a Cu-2.1wt%Be alloy

Ryoichi MONZEN[1], Tomoyuki HASEGAWA[2] and Chihiro WATANABE[3]

[1] Corresponding author, Division of Innovative Technology and Science, Kanazawa University, Kakuma-machi, Kanazawa 920-1192

TEL: +81-76-234-4678, FAX: +81-76-264-6495

Email: monzen@t.kanazawa-u.ac.jp

[2] Division of Mechanical Science and Engineering, Kanazawa University, Kakuma-machi, Kanazawa 920-1192

TEL: +81-76-234-4678, FAX: +81-76-264-6495

Email: hasegawa@metal.ms.t.kanazawa-u.ac.jp

[3] Division of Innovative Technology and Science, Kanazawa University, Kakuma-machi, Kanazawa 920-1192

TEL: +81-76-234-4677, FAX: +81-76-264-6495

Email: chihiro@t.kanazawa-u.ac.jp

Abstract

The influence of an applied stress on discontinuous precipitation (DP) in a Cu-2.1wt%Be alloy aged at 300ºC has been examined. A compressive stress accelerates the growth of DP cells, consisting of lamellae of the precipitated γ phase and the solute-depleted α phase, but a tensile stress does not essentially change it. The cell growth rates along the loading direction under the compressive and tensile stress are identical to those along the direction perpendicular to the loading direction under the same. Both the compressive and tensile stress have no influence on the incubation time to initiate DP. From measurements of the specimen length-change and investigations of the distribution of γ variants in cells in a particular case, specific γ variants among crystallographically equivalent ones are found to be formed, depending on the sense of the applied stress. This result, together with the dependence of the cell growth rate on the sense of the applied stress, can be well understood through the interaction energy between the external stress and the misfit strains of discontinuous γ precipitates.

Key words: Cu-Be alloy, discontinuous precipitation, applied stress, γ precipitates, orientation relationship, misfit, interaction energy

1. Introduction

Discontinuous precipitation (DP) involves the formation of a solute-depleted matrix phase (α) and a precipitate phase (γ) as a duplex transformation product behind a grain boundary advancing into a supersaturated matrix (α_0). This solid state phase transformation is so called because the changes in orientation and composition between the matrix phases (α and α_0) across the advancing boundary are discontinuous [1, 2].

The effect of an applied tensile stress on the growth rates of DP cells has been first studied by Sulonen [3, 4]. He observed that the applied tensile stress either enhanced or suppressed the DP at grain boundaries aligned either parallel or transverse to the loading direction in six binary alloys of Cu-Ag, Cu-Mg, Cu-Cd, Zn-Cu, Ag-Cu and Pb-Sn. An interpretation for this effect, which was based on an elastic strain energy interaction between the applied stress and the coherency stress field, was proposed. The predictions of his theory, which presumed the relative atomic radii of solute and matrix atoms, were in entire accord with his observed experimental results. Later, Hillert [5] has provided a quantitative treatment of the experimental results by Sulonen, based on the elastic interaction between the misfit stress field around the solute atoms ahead of the reaction front and applied tensile stress. The result of Sulonen and the analysis of Hillert have been widely quoted in support of the idea that a solute gradient exists in front of the discontinuous transformation interface [6, 7]. On the other hand, Dryden and Purdy [8] have proposed a model on the effect of external stress on DP kinetics, based on the inelastic interaction between the applied stress and misfit strain of the transformed regions. Guo et al. [9] have studied the influence of the applied stress on the morphology of DP in a Cu-Cd alloy.

In this study, the effects of an applied compressive or tensile stress on the growth rate and morphology of DP cells are investigated for a Cu-2.1wt%Be alloy aged 300°C. The DP cell in Cu-Be alloys consists of lamellae of the equilibrium γ phase (CuBe intermetallic) and

solute-depleted α phase (Cu-rich solid solution). Rod-shaped precipitates of the γ phase in DP cells exhibit an orientation relationship to Cu matrix of the α phase [10-12]. We have found that the growth rate of DP cells depends on the sense (tension or compression) of the applied stress, and the growth rates in the loading and the transverse directions are identical, different from the previous observations [3, 4, 6, 7, 9]. In addition, length-change measurements have been undertaken to estimate the average misfit strains along the loading and transverse directions, caused by the negative misfit strains between the α and γ phases, which were already determined from measurements of the length change and the lattice parameter on ageing using Cu-0.9wt%Be single crystals [13]. The dependences of the estimated misfit strains on the sense of the applied stress and the measured directions have revealed that specific γ variants among crystallographically equivalent ones are formed, depending on the sense of the applied stress. This is supported by the result of the distribution of the γ variants in cells formed under the applied stress in a specific case. This result, along with the effect of the sense of the applied stress on the cell growth rate, can be well explained in terms of the interaction energy due to the presence of negative misfit strains of the γ phase between the external stress and γ precipitate [14, 15].

2. Experimental

Ingots of a Cu-2.1wt%Be alloy were prepared by melting 99.99%Cu and a Cu-3.81wt%Be mother alloy. The alloy ingots were homogenized at 920 ºC for 48 h in a vacuum, cold-rolled to 50% reduction in thickness and then spark-cut into specimen strips. For compressive ageing, the specimens had a cross-section of 3 mm × 6 mm and a length of 6 mm. For tensile ageing, the specimens had the same cross-section but a gage length of 20 mm. All the specimens were solution-treated at 820 °C for 2 h in a vacuum, quenched into water and subsequently aged at 300 °C for various times either under an applied stress of 50 MPa (stress ageing) or under no

stress (free ageing). The applied stress of 50 MPa is about half of the yield strength of the solution-treated specimen at 300 °C. The average grain size after the solution treatment was about 50 μm.

Length changes ε_T on ageing were examined by measuring, with a micrometer, the distance between two scribed marks, about 5 mm and 10 mm apart for the compressive-stress-aged and tensile-stress-aged specimens, respectively. The length change is defined as $\varepsilon_T=(l-l_0)/l_0$, where l_0 and l are the length between the two marks before and after ageing at 300 °C for a time, respectively. The measurement accuracy of length change is in the order of 10^{-5} in strain. An X-ray analysis was performed to measure the lattice constants of the solution-treated and aged specimens. The diffractometer with a Cu target was used for the X-ray analysis.

Thin foils for transmission electron microscopy (TEM) observations were prepared by slicing the aged specimens with a spark cutter and by electropolishing using a solution of 67% methanol and 33% nitric acid at −30 °C and 6.5 V in a twin-jet electropolisher. Microscopy was carried out using a HITACHI H-9000NAR or a JEOL 2000EX microscope at an operation voltage of 300 or 200 kV.

3. Results

3.1. *Growth rate of cells*

When the Cu-Be supersaturated solid solution was transformed at 300ºC under no stress, DP cells developed equally and apparently randomly from grain boundaries. Even when a tensile and a compressive stress of 50 MPa were applied, this observation held, as exemplified in Figure 1. Figures 1a and b are optical microscopy images for the specimens, tensile-stress-aged and compressive-stress-aged at 300 ºC for 3 h. The width of cells in the tensile-stress-aged (TSA) specimen is smaller than that in the compressive-stress-aged (CSA) specimen. Figure 2

shows the cell width w against ageing time t for the specimens, free-aged (FA), compressive-stress-aged and tensile-stress-aged at 300ºC. About 100 DP cells were examined for each data point. A linear relationship exists between w and t for these specimens. It should be noted that the growth rates of cells along the loading direction (LD) and transverse direction (TD) are nearly the same for the TSA and CSA specimens. This result is in contrast with the results previously obtained [3, 4, 6, 7, 9] that the cell growth rate along the LD is different from that along the TD. In addition, the compressive stress accelerates the growth rate but the tensile stress does not essentially affect it. It is also seen that the applied stress has no influence on the incubation period to initiate DP (i.e. the intercept on the abscissa at w=0).

During ageing at 300 ºC up to 20 or 30 h, after which the surface of the CSA specimen or the FA and TSA specimens was occupied by DP cells, the continuous precipitation of fine Guinier-Preston (GP) zones, γ" and γ'_I occurred. However, the cell growth rate of DP was unchanged and linear in spite of the formation of GP zones, γ" and γ'_I, as seen in Figure 2. This is in agreement with the conclusion previously obtained by Tsubakino et al. [16] that fine GP zones and γ" and γ'_I precipitates do not affect the cell growth. The disc-shaped GP zones consist of monolayers of Be atoms on the Cu matrix $\{100\}_\alpha$ planes and transform continuously to the γ'_I phase via γ". These metastable phases are composed of alternate Be and Cu matrix layers parallel to $\{100\}_\alpha$ [17].

The effect of applied stress on DP was predicted qualitatively by Sulonen [3, 4] and analyzed quantitatively by Hillert [5]. When DP occurs in an elastically isotropic solid under an external stress σ and with a coherency strain δ in the solute diffusion zone abutting a grain boundary, the elastic strain energy ΔG in the coherent zone at the grain boundary perpendicular to the LD is expressed as [6]

$$\Delta G = \frac{E}{1-\nu}\delta^2 - \frac{2\nu}{1-\nu}\delta\sigma . \qquad (1)$$

If the grain boundary is parallel to the LD, the driving force for moving it (elastic strain energy) is written as

$$\Delta G = \frac{E}{1-\nu}\delta^2 + \delta\sigma \,. \qquad (2)$$

Since the sign of δ is minus in the present study [13], these equations predict that the growth of DP under tensile stress is faster along the LD than along the TD and the cell growth under compressive stress is reversed. However, this prediction is in conflict with the result of Figure 2. In addition, although Equation (1) indicates that tensile stress should enhance more the growth of DP along the LD than compressive stress, the situation is reserved. On the other hand, the prediction of Equation (2) that compressive stress promotes more the cell growth along the TD than tensile stress is in agreement with the result of Figure 2.

3.2. *Precipitation morphology*

The first critical step of the DP reaction in Cu-Be alloys is heterogeneous grain-boundary nucleation [11, 12]. Similar to our previous observation [12], boundary precipitation of the γ phase occurred before any significant boundary migration. Analyses of selected-area diffraction patterns (SADPs) of γ precipitates on boundaries in the FA, TSA and CSA specimens, taken using the zone axis parallel to $[110]_\alpha$ of one of the two abutting grains, revealed that the orientation relationship, $(1\bar{1}3)_\alpha$ // $(0\bar{1}3)_\gamma$; $[110]_\alpha$ // $[100]_\gamma$, was satisfied between the boundary γ precipitates and Cu matrix. This orientation relationship is in agreement with those for boundary precipitates reported by Bonfield and Edwards [10], Baumann et al. [11] and Monzen et al. [12].

The occurrence of DP reactions growing in two directions from one boundary was always observed. Figures 3a and b depict a TEM image of two DP cells growing in two directions from a boundary in the CSA specimen aged at 300 °C for 30 min and a $[110]_\alpha$ SADP

of a region labelled A in the upper cell. The LD is nearly parallel to the $[001]_\alpha$ direction of the matrix in the upper cell. Figure 3c is the schematic illustration of the previous SADP. In Figures 3b and c, the $[1\bar{1}1]_\alpha$ and $[1\bar{1}\bar{1}]_\alpha$ directions of the matrix in the region A are about 3º away from the $[0\bar{1}1]_\gamma$ and $[0\bar{1}\bar{1}]_\gamma$ directions of the upper and lower γ precipitates in the region A. Thus the upper or lower γ precipitates align with the Cu matrix in the region A according to the following orientation relationship: $(1\bar{1}3)_\alpha$ // $(0\bar{1}3)_\gamma$; $[110]_\alpha$ // $[100]_\gamma$ or $(1\bar{1}\bar{3})_\alpha$ // $(0\bar{1}\bar{3})_\gamma$; $[110]_\alpha$ // $[100]_\gamma$. The orientation relationship is coincident with those for DP reported by Bonfield and Edwards [10] and Monzen et al. [12]. The γ precipitates in all cells examined exhibited the orientation relationship to the Cu matrix, and had the $\{113\}_\alpha$ habit plane, as seen in Figure 3a. The orientation of the habit plane was determined by tilting the precipitates until the facet habit plane was accurately edge-on. In addition, the growth direction of the γ precipitates was determined, using TEM images from $<110>_\alpha$ and $<\bar{1}13>_\alpha$, to be approximately $<3\bar{3}2>_\alpha$. The direction is in agreement with the elongated direction of γ precipitates in a Cu-0.9wt%Be single crystal [17].

In the above orientation relationship, one directional parallelism has two planar parallelisms as represented. Since there are six independent directional parallelisms, the orientation relationship has twelve variants in total. The twelve variants of γ precipitates are divided into three groups I, II and III, as shown in the left column of Table 1. The variants I-1~4, II-1~4 and III-1~4 have the misfit strains of $\varepsilon_{11}=\varepsilon_{22}=-0.03$ and $\varepsilon_{33}=-0.08$, $\varepsilon_{11}=\varepsilon_{33}=-0.03$ and $\varepsilon_{22}=-0.08$, and $\varepsilon_{22}=\varepsilon_{33}=-0.03$ and $\varepsilon_{11}=-0.08$ [13]. The misfit strains ε_{11}, ε_{22} and ε_{33} are described on the coordinate of the matrix crystal with x_1 // [100], x_2 // [010] and x_3 // [001].

In the present Cu-Be alloy aged at 300ºC, the cell growth in two directions from one grain boundary always took place, as shown in Figure 3a. Baumann et al. [11] have shown that, in a Cu-1.8wt%Be-0.25wt%Co alloy aged at low temperatures below about 400 ºC, as a consequence of the growth in opposite directions from the initial grain-boundary configuration,

the double-seam DP morphology occurs. In the FA, TSA and CSA specimens also, the double-seam morphology was always observed. Figures 4a and b show scanning electron microscopy (SEM) images of the double-seam morphology in the CSA specimen. The cell growth directions in Figures 4a and b are nearly parallel to the LD and TD, respectively. Precipitates in each DP cell are elongated along various directions, independent of the cell growth direction.

3.3. *Specimen length-change*

Figure 5 presents the length change ε_T along the LD and TD, plotted as a function of ageing time t for the FA, CSA and TSA specimens on ageing at 300 °C for various times up to 80 h (2.88×10^5 s). In the early stage of ageing up to 30 min (1.8×10^3 s), length change along the LD and TD for the FA, CSA and TSA specimens shows no essential change. On ageing for 30 min, γ'' precipitates primarily existed within the grain interiors, which consisted of a two Be-layer structure separated by a matrix layer parallel to $\{001\}_\alpha$ [13, 17]. DP reactions began to occur after ageing for 30 min and proceeded until the surface of the CSA specimen or the FA and TSA specimens was filled with DP cells after 20 or 30 h (7.2×10^4 or 1.08×10^5 s). As the amount of DP cells increased, length change along the LD or TD for the CSA specimen rapidly decreased or slightly increased up to 20 h and became constant, whereas length change along the LD or TD for the TSA specimen exhibited initially a slight increase or a rapid decrease and then a plateau behaviour after 30 h. When values of ε_T along several directions for the specimen, free-aged for 2 and 80 h were measured, the values for each time were identical within experimental error. In other words, there existed no anisotropy in length change of the FA specimen. In Figure 5, the FA specimen shows a decrease in length change and then a constant value after 30 h. It should be noted that length change along the LD for the TSA or CSA specimen exhibits no change after ageing for 30 min and during ageing from 30 to 80 h. On ageing for 5 h (1.8×10^4 s), γ'_I precipitates were mainly observed within the grain interiors,

which were composed of five to eight Be-layers parallel to $\{100\}_\alpha$ [13, 17]. The result of microhardness tests revealed that the Vickers hardness of grain interiors after ageing for 5 h was larger than that after ageing for 30 min but smaller than the hardness of DP cells after ageing for 5 h, and the hardness of the cells was constant during ageing up to 80 h. These results indicate that the creep strain due to dislocation motion does not contribute to the length change.

In our previous study [13], we have shown that the length-change behaviour of Cu-1.8wt%Be-0.2wt%Co alloy polycrystals during ageing at 500°C, at which continuous and discontinuous precipitation occurs simultaneously, is well represented by the equation:

$$\varepsilon_{\mathrm{T}} = \frac{f\left(\varepsilon_{11} + \varepsilon_{22} + \varepsilon_{33}\right)}{3} + (1 - f)\varepsilon_l, \tag{3}$$

where f is the volume fraction of precipitates and ε_{11}, ε_{22} ($=\varepsilon_{11}$) and ε_{33} are the misfit strains of GP zones and γ'', γ'_{I}, γ' and γ precipitates. The misfit strains ε_{11}, ε_{22} and ε_{33} are described on the coordinate of the matrix crystal with x_1 // [100], x_2 // [010] and x_3 // [001]. ε_l is the dimensional change due to the loss of Be solute atoms from the solid solution and given by

$$\varepsilon_l = \frac{a - a_0}{a_0}, \tag{4}$$

where a_0 and a are the lattice parameters of specimens before and after ageing. Equation (3) is applicable when each variant of GP zone and each phase, for instance, each γ variant in Table 1 is equally present in the Cu matrix [13]. Equation (3) also indicates that there is no anisotropy in the length change. In fact, the length change of the FA specimen showed no anisotropy, as mentioned before.

We will estimate the average misfit strain ε_{a}, which is obtained from Equation (3) by replacing $(\varepsilon_{11}+\varepsilon_{22}+\varepsilon_{33})/3$ by ε_{a}, when the surfaces of the FA, CSA and TSA specimens were covered with DP cells. The value of f=0.20 was determined by applying the values of

a_0=0.3574nm and a=0.3612nm to the experimental data regarding the dependence of the lattice parameter on Be concentration [18]. The average misfit strains ε_{aL} and ε_{aT} along the LD and TD for the CSA, TSA and FA specimens were estimated from the values of ε_T in Figure 5, f and ε_i. The value of $(1-f)\varepsilon_i$ caused by the decrease in Be solute atoms in the matrix after DP is estimated as 8.5 x 10^{-3} from Equation (4). For example, the value of $f\varepsilon_a$ based on the existence of the γ phase with negative misfits in the FA specimen is calculated as −9.7 x 10^{-3} from the value of ε_T in Figure 5 and Equation (3). The average misfit strains for the CSA, TSA and FA specimens, thus obtained, are summarized in Table 2. The calculated value of ε_a for the FA specimen using the values of ε_{11}, ε_{22} and ε_{33} described in Section 3.2 is −0.047, which is in good agreement with the experimentally obtained value of ε_a=−0.048 in Table 2. For the CSA specimen, $-0.08 < \varepsilon_{aL} < -0.048 < \varepsilon_{aT} < -0.03$, and, for the TSA specimen, $-0.08 < \varepsilon_{aT} < -0.048 < \varepsilon_{aL} < -0.03$. This indicates that particular γ variants out of crystallographically equivalent ones are formed, depending on the sense of the applied stress. The distribution of γ variants in the CSA and TSA specimens will be examined in a specific case below.

3.4 *Distribution of γ variants*

We selected the DP cells in which the $[001]_\alpha$ direction of the matrix was nearly parallel to the LD, and determined the orientations of the γ precipitates in the cells, using the electron beam parallel to $[110]_\alpha$ or $[\bar{1}10]_\alpha$ in the cells. For example, the lower and upper γ precipitates in the region A in Figure 3a have the orientations I-1 and I-2. If no reflections from a γ precipitate are observed using the zone axis parallel to $[011]_\alpha$ or $[0\bar{1}1]_\alpha$, the γ precipitate has one of the orientations II-1~4 and III-1~4. Discontinuous γ precipitates formed behind initial grain-boundary migration, such as γ precipitates in a region labelled B in Figure 3a, was excluded, since such γ variants are unlikely to be a reflection of the direct effect of applied stress, as will

be discussed in Section 4. The γ precipitates in the region B did not have the orientations I-1~4. More than 200 rod-shaped precipitates were examined in DP cells after the double seams were formed. The final result of the distribution of the variants formed under tensile stress and compressive stress is summarized in Table 2. In the CSA specimen, the variants I-1~4 are preferentially formed, whereas these variants are scarcely observed in the TSA specimen.

4. Discussion

As mentioned in Section 3.1, the results in Figure 2 that the cell growth rate under compressive stress is faster than that under tensile stress and the cell growth rate along the LD is the same as that along the TD cannot be explained from Equations (1) and (2). The origin of the dependences of the growth rate of DP (Figure 2), the formation of particular variants of γ precipitates in cells (Table 1) and the average misfit strains in the LD and TD (Table 2) on the sense of the applied stress can be understood to arise through the interaction energy due to the presence of negative misfit strain ε_{ij} (stress-free transformation strain) between a γ precipitate and an external stress σ_{ij}. That is, the cause of the present results is understood as due to the work done by the external stress during the growth of discontinuous γ precipitates. The interaction energy ΔE per unit volume of the γ precipitate is expressed as [12, 13]

$$\Delta E = -\sigma_{ij}\varepsilon_{ij} \qquad (5)$$

This equation predicts that the growth of γ precipitates, namely DP cells is promoted by applied compressive stress because of $\varepsilon_{ij} < 0$ and, as a result, the growth of cells under compressive stress is easier than that under tensile stress. This prediction is in agreement with the result of Figure 2. Also, it may be expected from Equation (5) that, when the stress axis is parallel to the $[001]_\alpha$ direction, since the values of ε_{33} along $[001]_\alpha$ for the γ variants I-1~4 and the variants II-1~4 and III-1~4 in Table 1 are −0.08 and −0.03, respectively, compressive stress enhances

formation and growth of the γ variants I-1~4 and tensile stress particularly suppresses formation of the variants I-1~4. This is coincident with the observed frequencies of γ variants in Table 1. Moreover, Equation (5) predicts that, for the CSA specimen, the average misfit strain ε_{aL} along the LD is between ε_{33}=−0.08 and ε_a=−0.048 for the FA specimen, and the value of ε_{aT} along the TD is between −0.048 and −0.03, and, for the TSA specimen, $-0.08 < \varepsilon_{aT} < -0.048 < \varepsilon_{aL} < -0.03$. This is also the case, as shown in Table 2.

In the previous and present studies [11, 12], precipitation of the γ phase takes place first at grain boundaries and then the boundaries migrate. Initial boundary migration occurs locally between two existing γ precipitates, leaving the precipitates embedded in the grain in which the habit plane with a low interface-energy forms on both sides of the precipitates [12]. This behaviour is similar to that predicted by Tu and Turnbull [19, 20]. In the pucker mechanism proposed by Tu and Turnbull, the driving force for initial boundary migration is provided by the reduction in total interface energy of a boundary precipitate. There also is another mechanism for the nucleation of DP suggested by Fournelle and Clark [21]. In this mechanism, DP can develop from an initially unoccupied grain-boundary, boundary migration due to recrystallization and/or grain growth forces initiates the DP reaction and then boundary precipitates form. Subsequently the mechanism involves the bowing of a free segment of the mobile grain boundary between the adjacent pinning centres. Although direct evidence for this mechanism could not be provided in the present study, the mechanism is capable of operating. Even if either mechanism operates in this system, the formation of initial discontinuous precipitates, namely the incubation period to initiate DP should be unaffected by the external stress. In fact, this holds true, as shown in Figure 2. In addition, as exemplified in the region B in Figure 3a, the initial discontinuous γ precipitates in the CSA specimen seldom had the orientations I-1~4 which is favorable under compression from Equation (5).

As can be seen in the upper cell in Figure 3a, the growth of the γ precipitates in the

region B, having not the orientations I-1~4 which are favorable in compression in Table 1, is discontinued, and then the γ precipitates with the orientations I-1 and 2 are newly formed. In this case, boundary precipitation must have occurred during boundary migration, and subsequently only boundary γ precipitates of the orientations I-1 and 2 must have been elongated with boundary migration, since generally the grain boundary has several variants of the γ precipitates [12]. In this way, the γ variants which are favored under the applied stress may have been selected and grown.

When the stress axis is along the $[001]_\alpha$ direction of the matrix in DP cells, as shown in Table 1, the four variants I-1~4 among crystallographically equivalent twelve ones were primarily observed in the CSA specimen, while the discontinuous γ precipitates in the TSA specimen scarcely had the four orientations. This could be understood by considering that the applied compressive stress assists the growth of γ precipitates with the four orientations and the applied tensile stress hinders particularly the growth of the four variants. If this idea is followed, in principle, at least four variants exist in a DP cell in both of the CSA and TSA specimens, and thus there should be more than four growth directions of γ precipitates in any cell in the specimens. In fact, the discontinuous precipitates in the specimens grew in various <332> directions, regardless of the cell growth direction, as exemplified in Figures 4a and b. This is probably the reason why the growth rates along the LD and TD are the same for the CSA and TSA specimens.

5. Conclusions

(1) Application of compressive stress during ageing at 300ºC promotes the growth of discontinuous precipitation (DP) cells in a Cu-2.1wt%Be alloy, but tensile stress does not essentially affect the same. The growth rates along the loading and the transverse directions are identical for the specimens, compressive-stress-aged (CSA) and tensile-stress-aged (TSA). The

incubation period to initiate DP is unaffected by the applied stress.

(2) From measurements of the length change and the lattice parameter, the average misfit strains along the loading and the transverse directions, based on the misfit strains of discontinuous γ precipitates, have been estimated for the CSA and TSA specimens. The estimates reveal that specific γ variants among crystallographically equivalent ones are preferentially formed, depending on the sense of the applied stress. This is supported by the result of the distribution of the γ variants in DP cells formed under the applied stress in a special case.

(3) The dependences of the cell growth rate and the formation of specific γ variants on the sense of the applied stress can be understood through the interaction energy due to the presence of negative misfit strains between the applied stress and discontinuous γ precipitate.

Acknowledgements

A part of this work was conducted in the Kyoto-Advanced Nanotechnology Network, supported by the "Nanotechnology Network" of the Ministry of Education, Culture, Sports, Science and Technology (MEXT), Japan. This work was also partially supported by a Grant-in-Aid for Science Research from The Ministry of Education, Culture, Sports and Technology under Grant No.19560742.

References

[1] D. B. Williams and E. A. Butler, Inter. Met. Rev. 26 (1981) p.153.

[2] I. Manna, S. K. Pabi and W. Gust, Inter. Mater. Rev. 46 (2001) p.53.

[3] M. S. Sulonen, Acta Metall. 12 (1964) p.749.

[4] M. S. Sulonen, Acta Polytec. Scand. (a) 38 (1964) p.3.

[5] M. Hillert, Metal. Trans. 3 (1972) p.2729.

[6] Y. H. Chung, M. C. Shin and D. Y. Yoon, Acta Metall. Mater. 40 (1992) p.2177.

[7] Y. G. Na, C. D. Yim, S. C. Park and K. S. Shin, Mater. Sci. Forum 419-422 (2003) p.285.

[8] J. R. Dryden and G. R. Purdy, Acta Metall. Mater. 38 (1990) p.1255.

[9] W. Guo, J. R. Dryden and G. R. Purdy, Acta Metall. Mater. 41 (1993) p.1183.

[10] W. Bonfield and B. C. Edwards, J Mater. Sci. 9 (1974) p.409.

[11] S. F. Baumann, J. Michael and D. B. Williams, Acta Metall. 29 (1981) p.1343.

[12] R. Monzen, C. Watanabe, D. Mino and S. Saida, Acta Mater. 53 (2005) p.1253.

[13] C. Watanabe, T. Sakai and R. Monzen, Phil. Mag. A 88 (2008) p.1401.

[14] J. D. Eshelby, Proc. R. Soc. (a) 241 (1957), p.376.

[15] J. D. Eshelby, Proc. R. Soc. (a) 252 (1959), p.561.

[16] H. Tsubakino, R. Nozato and A. Yamamoto, Mater. Sci. Tech. 9 (1993) p.288.

[17] R. Monzen, T. Seo, T. Sakai and C. Watanabe, Mater. Trans. 47 (2006) p.2925.

[18] H. Tanimura and G. Wassermann, Z. Metallk. 25 (1933) p.179.

[19] K. N. Tu and D. Turnbull, Acta Metall. 15 (1967) p.369.

[20] K. N. Tu and D. Turnbull, Acta Metall. 15 (1967) p.1317.

[21] R. A. Fournelle and J. B. Clark, Metall. Trans. 3(1972) p.2757.

Tables with captions

Table 1 Observed frequencies of γ variants in the DP cells particularly selected for the specimens, tensile-stress-aged and compressive-stress-aged. The stress axis is along the $[001]_\alpha$ direction of the Cu matrix in the DP cells.

Variant notation	Variant		Obserbed frequency Compression	Tension	Misfit
I – 1	$(1\bar{1}\bar{3})_\alpha$ // $(0\bar{1}\bar{3})_\gamma$	$[110]_\alpha$ // $[100]_\gamma$	90%	12%	–0.08
2	$(1\bar{1}3)_\alpha$ // $(0\bar{1}3)_\gamma$				
3	$(11\bar{3})_\alpha$ // $(10\bar{3})_\gamma$	$[1\bar{1}0]_\alpha$ // $[0\bar{1}0]_\gamma$			
4	$(113)_\alpha$ // $(103)_\gamma$				
II – 1	$(\bar{1}31)_\alpha$ // $(130)_\gamma$	$[101]_\alpha$ // $[001]_\gamma$	10%	88%	–0.03
2	$(13\bar{1})_\alpha$ // $(1\bar{3}0)_\gamma$				
3	$(\bar{1}3\bar{1})_\alpha$ // $(03\bar{1})_\gamma$	$[10\bar{1}]_\alpha$ // $[\bar{1}00]_\gamma$			
4	$(131)_\alpha$ // $(0\bar{3}\bar{1})_\gamma$				
III – 1	$(3\bar{1}1)_\alpha$ // $(301)_\gamma$	$[011]_\alpha$ // $[010]_\gamma$			
2	$(31\bar{1})_\alpha$ // $(\bar{3}01)_\gamma$				
3	$(3\bar{1}\bar{1})_\alpha$ // $(\bar{3}\bar{1}0)_\gamma$	$[01\bar{1}]_\alpha$ // $[00\bar{1}]_\gamma$			
4	$(311)_\alpha$ // $(3\bar{1}0)_\gamma$				

Table 2 Average misfit strains ε_{aL} and ε_{aT} along the loading direction and transverse direction, obtained by length-change measurements, for the specimens, tensile-stress aged (TSA), compressive-stress aged (CSA) and free-aged (FA).

Specimen	ε_{aL}	ε_{aT}
TSA	–0.039	–0.061
CSA	–0.065	–0.041
FA	–0.048	

Figure Captions

Fig. 1 Optical micrographs of (a) tensile-stress-aged and (b) compressive-stress-aged specimens. Ageing was carried out at 300 °C for 3 h. The arrows in (a) and (b) indicate the loading direction.

Fig. 2 Variation in the width of DP cells during free ageing, tensile-stress ageing and compressive-stress ageing at 300 °C. Representative error bars are shown.

Fig. 3 (a) TEM image of the specimen, compressive-stress-aged at 300 °C for 30 min. The arrow in (a) indicates the loading direction. (b) $[110]_{\alpha}$ SADP corresponding to a region labelled A in (a). (c) Schematic illustration of the previous SADP. ●=I-1 γ reflections, ○=I-2 γ reflections.

Fig. 4 SEM images of double seams of DP cells growing in (a) the loading direction and (b) the transverse direction for the specimen, compressive-stress-aged at 300°C for 1h. The arrows in (a) and (b) indicate the loading direction. RF=Reaction Front.

Fig. 5 Variation in the specimen length-change during free ageing, tensile-stress ageing and compressive-stress ageing at 300 °C. Representative error bars are shown.

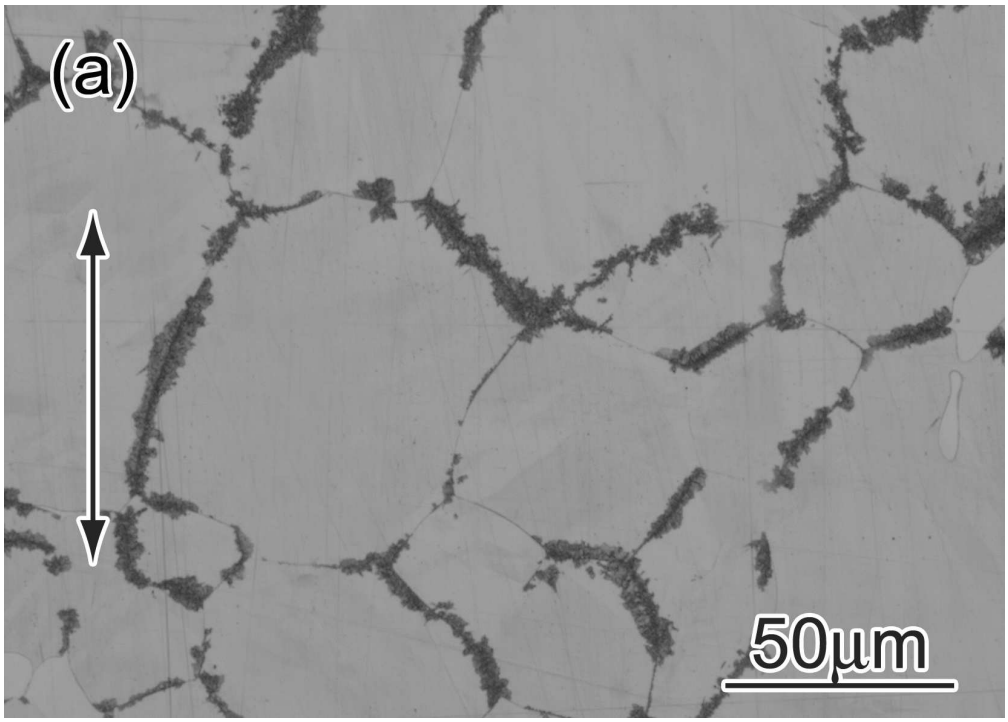

Fig. 1 Optical micrographs of (a) tensile-stress-aged and (b) compressive-stress-aged specimens. Ageing was carried out at 300°C for 3h. The arrows in (a) and (b) indicate the loading direction.
70x49mm (600 x 600 DPI)

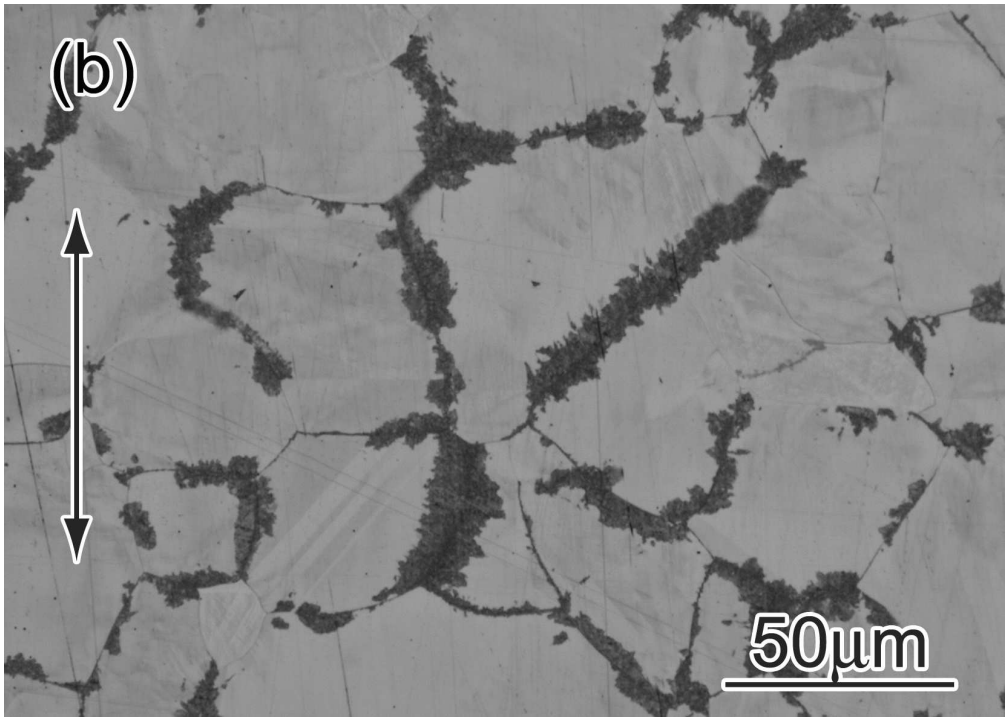

Fig. 1 Optical micrographs of (a) tensile-stress-aged and (b) compressive-stress-aged specimens. Ageing was carried out at 300°C for 3h. The arrows in (a) and (b) indicate the loading direction.
70x49mm (600 x 600 DPI)

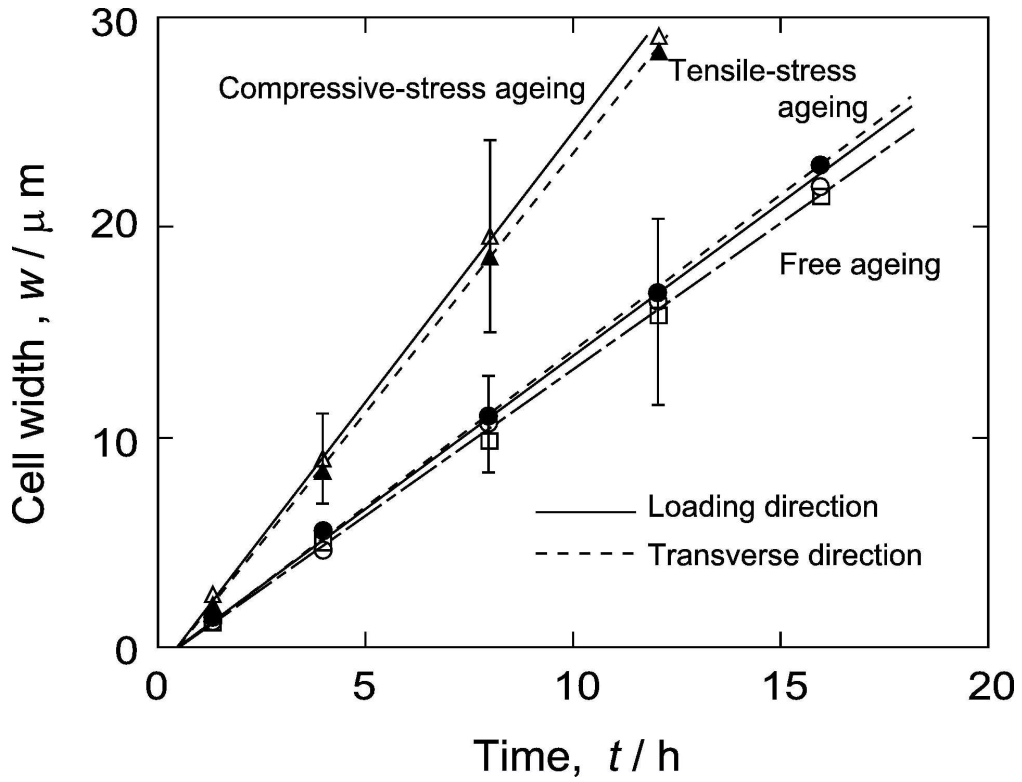

Fig. 2 Variation in the width of DP cells during free ageing, tensile-stress ageing and compressive-stress ageing at 300 °C. Representative error bars are shown.
163x125mm (600 x 600 DPI)

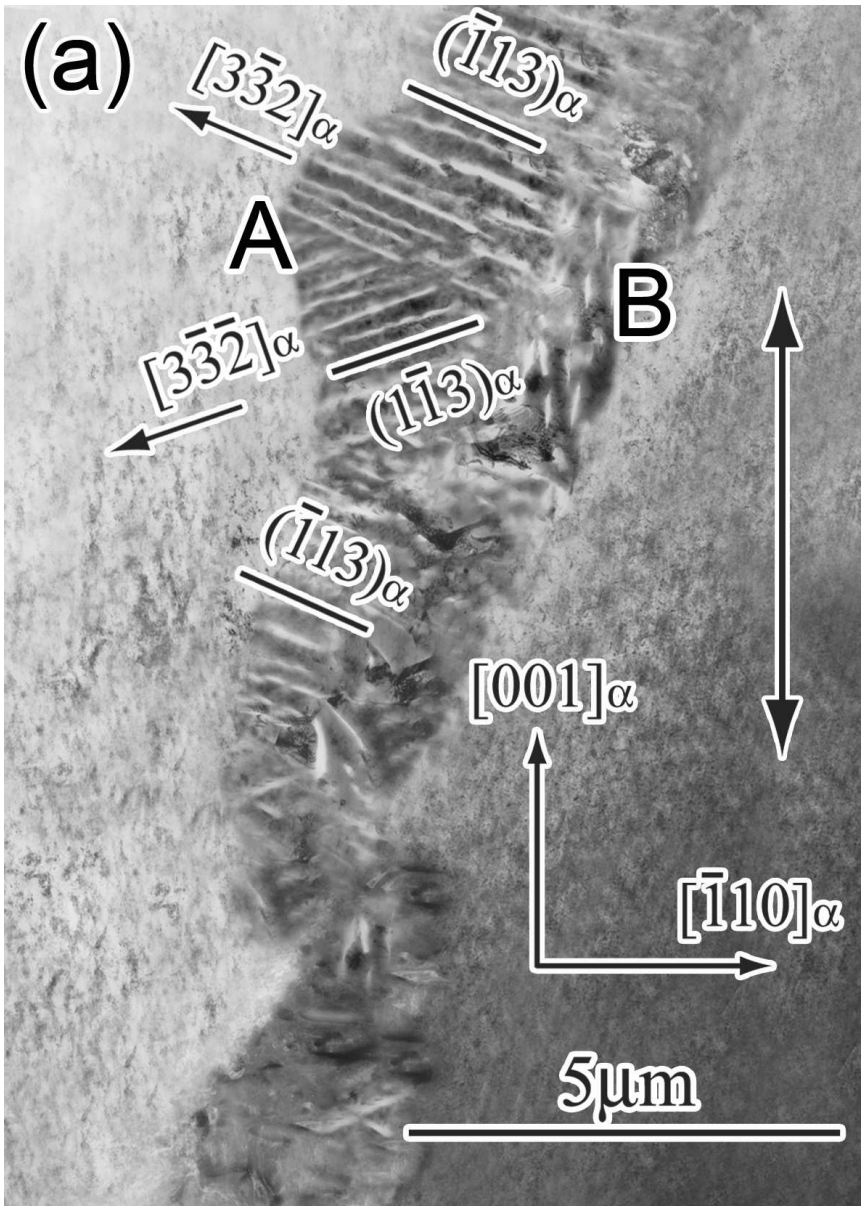

Fig. 3 (a) TEM image of the specimen, compressive-stress aged at 300o°C for 30min. The arrow in (a) indicates the loading direction. (b) [110]α SADP corresponding to a region labelled A in (a). (c) Schematic illustration of the previous SADP. ●=I-1 γ reflections, ○=I-2 γ reflections.
49x70mm (600 x 600 DPI)

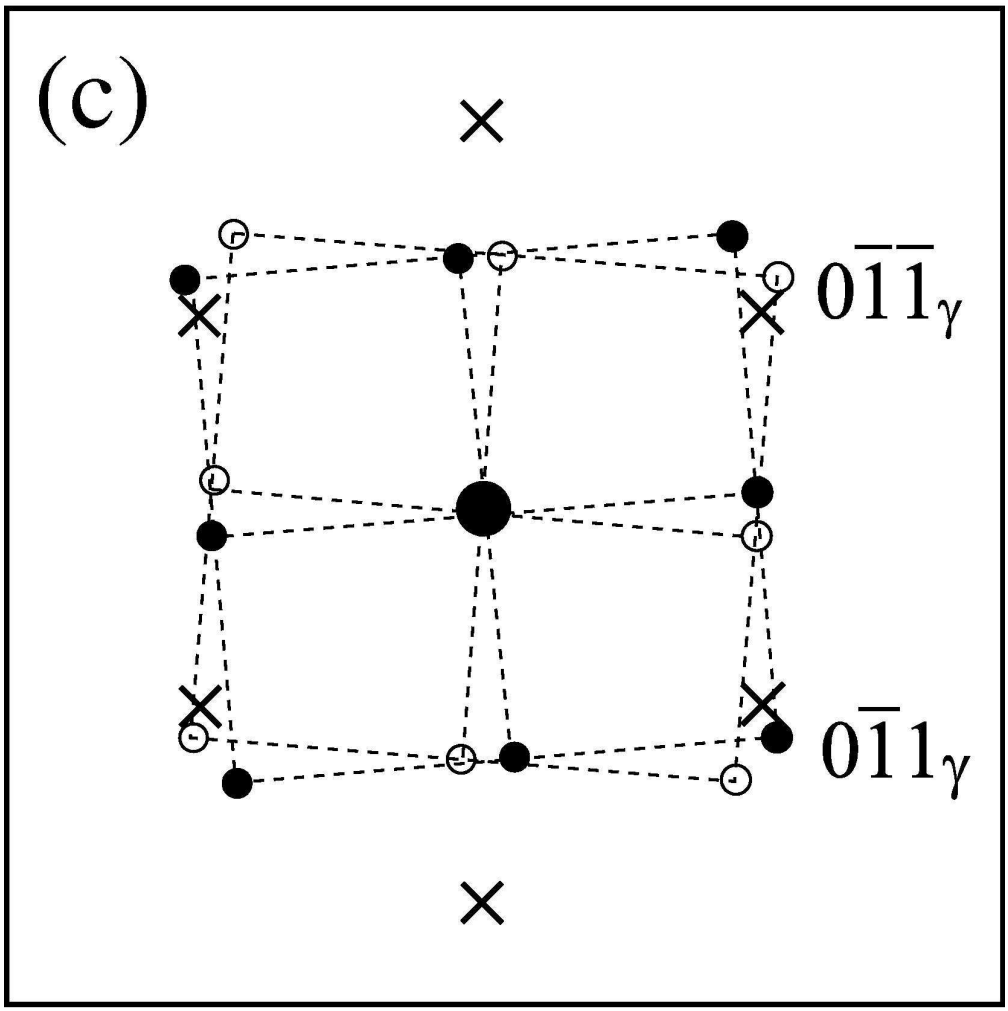

Fig. 3 (a) TEM image of the specimen, compressive-stress aged at 300o°C for 30min. The arrow in (a) indicates the loading direction. (b) [110]α SADP corresponding to a region labelled A in (a). (c) Schematic illustration of the previous SADP. ●=I-1 γ reflections, ○=I-2 γ reflections.
70x70mm (600 x 600 DPI)

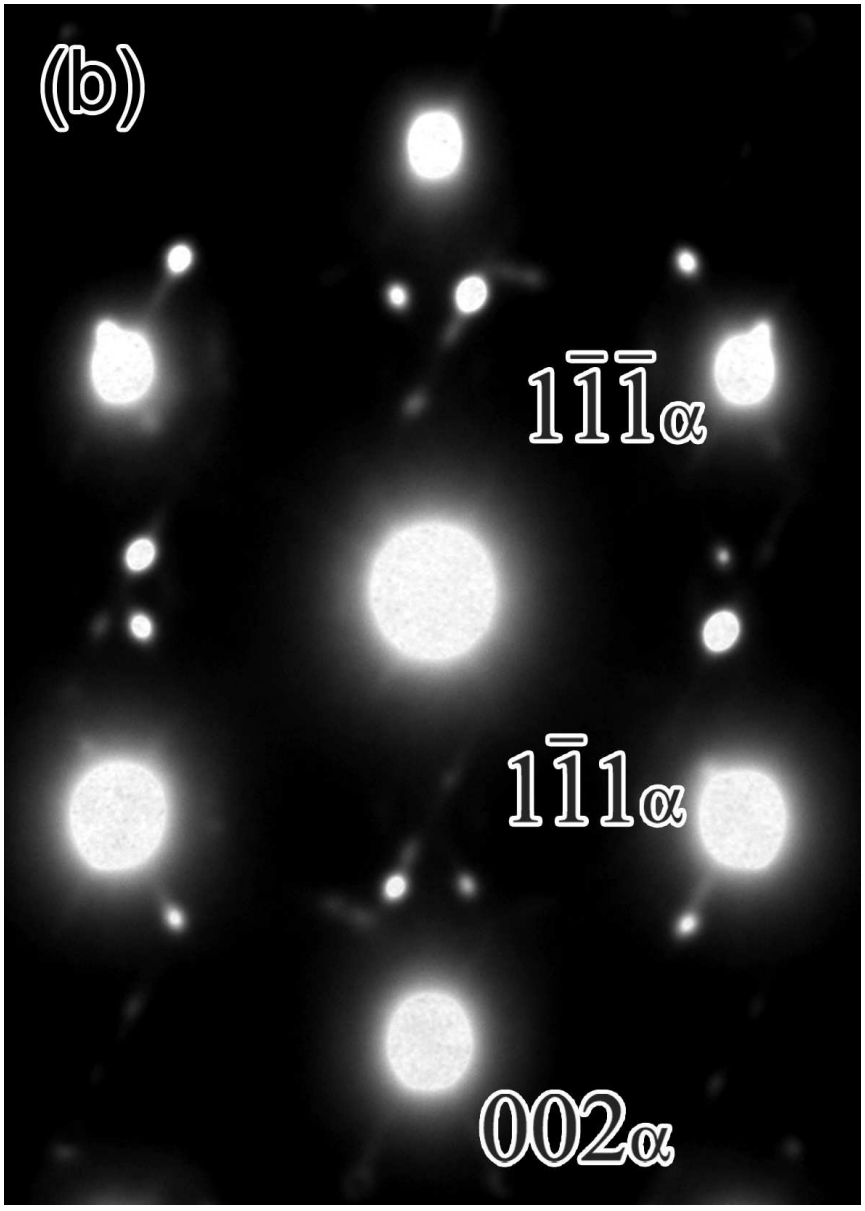

Fig. 3 (a) TEM image of the specimen, compressive-stress aged at 300o°C for 30min. The arrow in (a) indicates the loading direction. (b) [110]α SADP corresponding to a region labelled A in (a). (c) Schematic illustration of the previous SADP. ●=I-1 γ reflections, ○=I-2 γ reflections.
49x70mm (600 x 600 DPI)

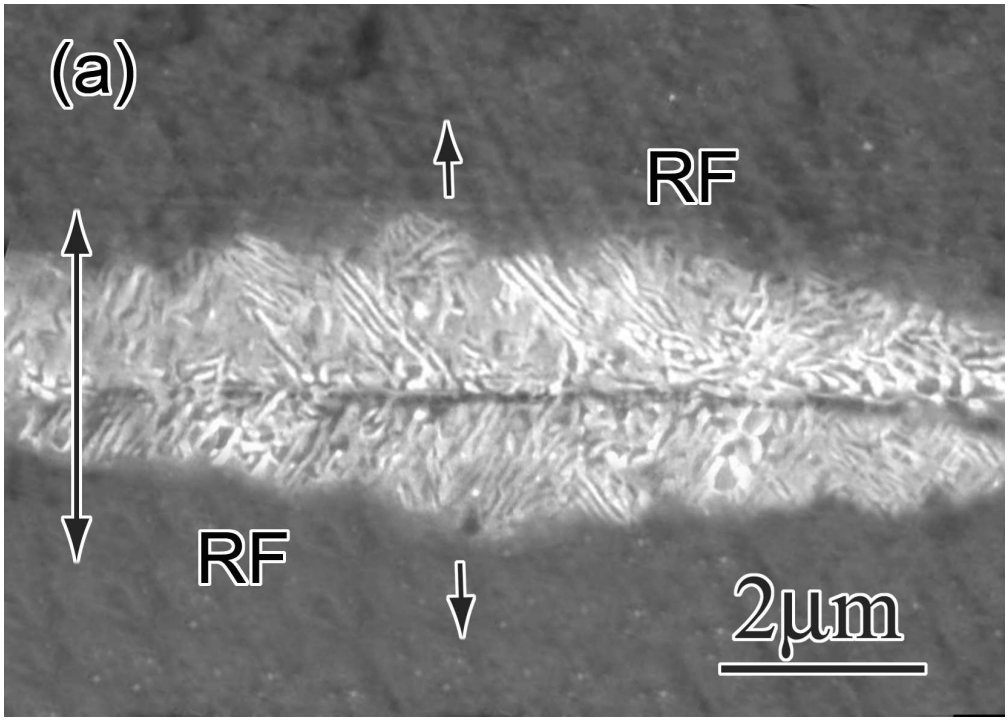

Fig. 4 SEM images of double seams of DP cells growing towards (a) the loading direction and (b) the transverse direction for the specimen, compressive-stress-aged at 300°C for 1h. The arrows in (a) and (b) indicate the loading direction. RF=Reaction Front.
70x49mm (600 x 600 DPI)

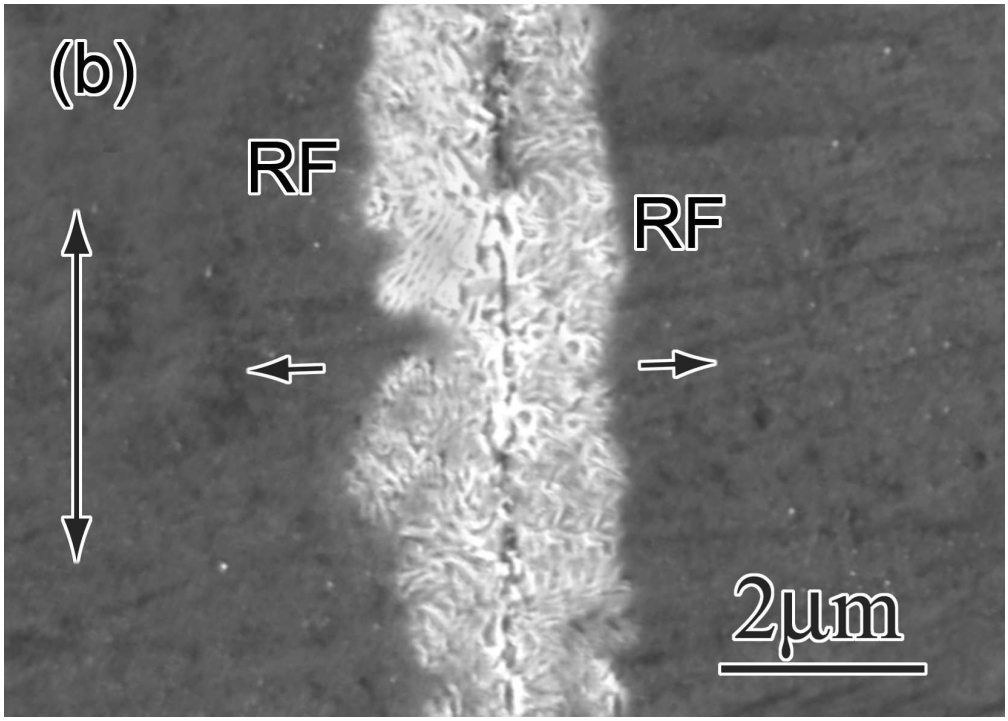

Fig. 4 SEM images of double seams of DP cells growing towards (a) the loading direction and (b) the transverse direction for the specimen, compressive-stress-aged at 300°C for 1h. The arrows in (a) and (b) indicate the loading direction. RF=Reaction Front.
70x49mm (600 x 600 DPI)

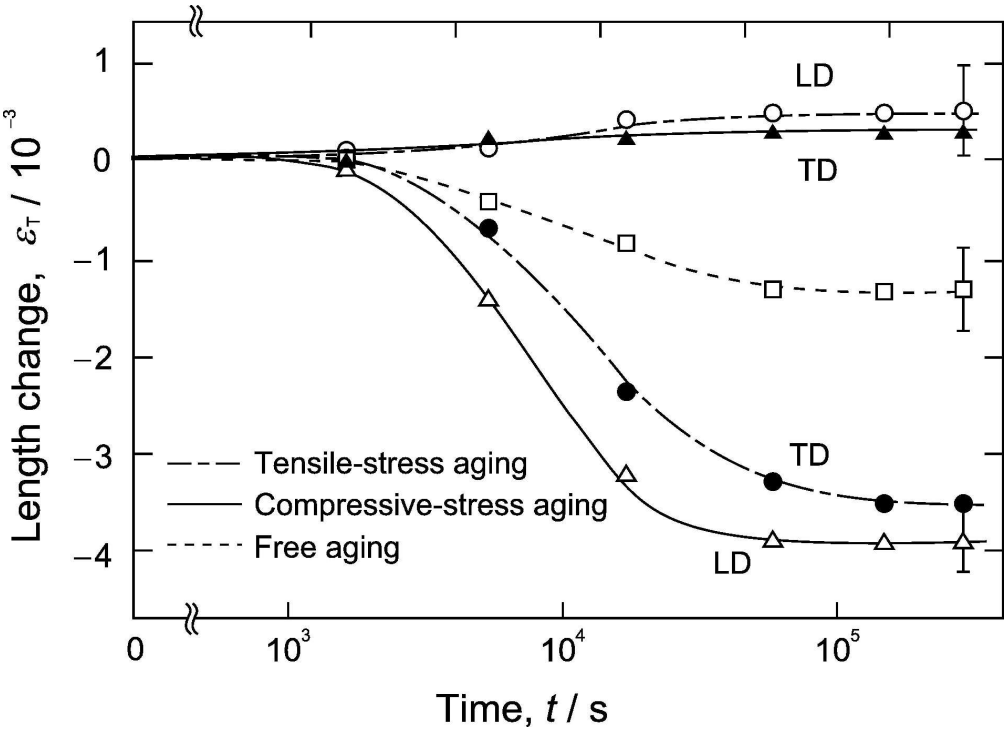

Fig. 5 Variation in the specimen length-change during free ageing, tensile-stress ageing and compressive-stress ageing at 300 °C. Representative error bars are shown.
161x116mm (600 x 600 DPI)

Variant notation	Variant		Obserbed frequency Compression	Tension	Misfit
I – 1	$(1\bar{1}\bar{3})_\alpha$ // $(0\bar{1}\bar{3})_\gamma$	$[110]_\alpha$ // $[100]_\gamma$	90%	12%	– 0.08
2	$(1\bar{1}3)_\alpha$ // $(0\bar{1}3)_\gamma$				
3	$(11\bar{3})_\alpha$ // $(10\bar{3})_\gamma$	$[1\bar{1}0]_\alpha$ // $[0\bar{1}0]_\gamma$			
4	$(113)_\alpha$ // $(103)_\gamma$				
II – 1	$(\bar{1}31)_\alpha$ // $(130)_\gamma$	$[101]_\alpha$ // $[001]_\gamma$	10%	88%	– 0.03
2	$(13\bar{1})_\alpha$ // $(1\bar{3}0)_\gamma$				
3	$(\bar{1}3\bar{1})_\alpha$ // $(03\bar{1})_\gamma$	$[10\bar{1}]_\alpha$ // $[\bar{1}00]_\gamma$			
4	$(131)_\alpha$ // $(0\bar{3}\bar{1})_\gamma$				
III – 1	$(3\bar{1}1)_\alpha$ // $(301)_\gamma$	$[011]_\alpha$ // $[010]_\gamma$			
2	$(31\bar{1})_\alpha$ // $(\bar{3}01)_\gamma$				
3	$(3\bar{1}\bar{1})_\alpha$ // $(\bar{3}\bar{1}0)_\gamma$	$[01\bar{1}]_\alpha$ // $[00\bar{1}]_\gamma$			
4	$(311)_\alpha$ // $(3\bar{1}0)_\gamma$				

Table 1 Observed frequencies of γ variants in the DP cells particularly selected for the specimens, tensile-stress-aged and compressive-stress-aged. The stress axis is parallel to the [001]αdirection of the Cu matrix in the DP cells.
188x102mm (600 x 600 DPI)

Specimen	ε_{aL}	ε_{aT}
TSA	−0.039	−0.061
CSA	−0.065	−0.041
FA	−0.048	

Table 2 Average misfit strains ε_{aL} and ε_{aT} along the loading direction and transverse direction, obtained by length-change measurements, for the specimens, tensile-stress aged (TSA), compressive-stress aged (CSA) and free-aged (FA).
140x42mm (600 x 600 DPI)